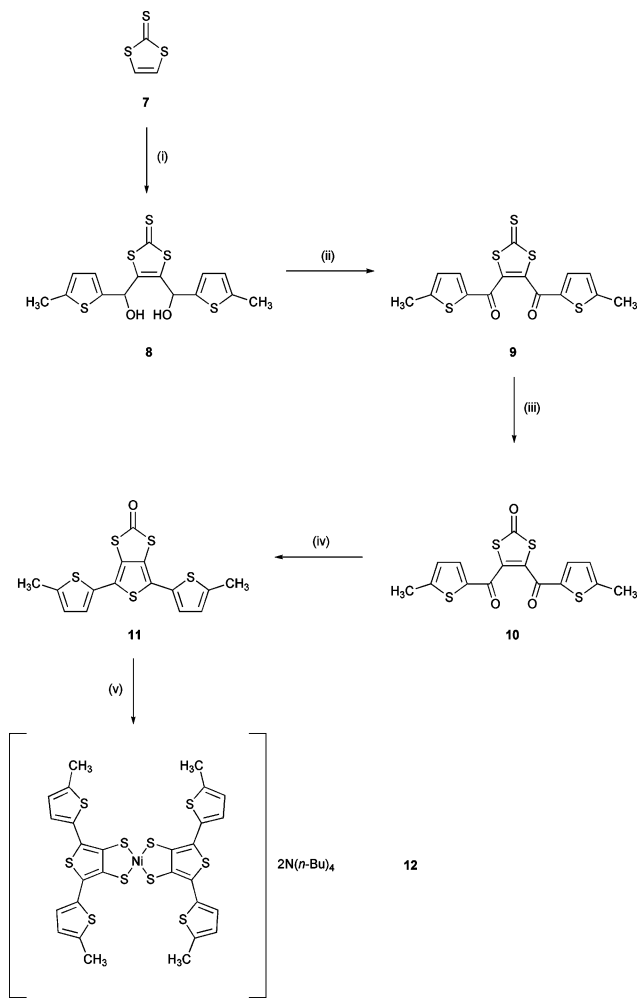




NiCl<sub>2</sub> and *n*-Bu<sub>4</sub>NBr gave the corresponding nickel bis(dithiolene) complex **3** (50% yield), after precipitation with petroleum ether (boiling range 40–60 °C). Similarly, the Pd(II) analogue (**4**) was obtained from **2** by addition of Na<sub>2</sub>[PdCl<sub>4</sub>] and Et<sub>4</sub>NBr (49% yield). Gold(III) complexes, **5** and **6**, were isolated from the reaction of **2** with PPN[AuCl<sub>4</sub>] (38% yield) and *n*-Bu<sub>4</sub>N[AuBr<sub>4</sub>] (55% yield), respectively (PPN = N(PPh<sub>3</sub>)<sub>2</sub>).

The synthesis of a derivative of **3**, end-capped with four methyl groups, is illustrated in Scheme 2. The route follows the same strategy adopted for the preparation of terthiophene **1**,<sup>20</sup> which uses vinylene trithiocarbonate **7** as the starting material. Monolithiation of **7** with one equivalent of lithium diisopropylamide (LDA) was followed by the addition of 5-methylthiophene-2-carboxaldehyde and the whole procedure was repeated a second time. The resulting diol (**8**) was obtained after aqueous work-up and reacted immediately without purification with MnO<sub>2</sub> to afford diketone **9** (67% yield from **7**). Conversion of the trithiocarbonyl functionality to the dithiooxone (**10**, 72%) was accomplished by the reaction of mercuric acetate. Phosphorus pentasulfide was used to cyclise compound **10** and the resulting end-capped terthiophene (**11**) was isolated in 52% yield. Finally, **12**



**Scheme 2** Reagents and conditions: (i) LDA, -78 °C, THF, 5-methylthiophene-2-carboxaldehyde, then repeat; (ii) MnO<sub>2</sub>, CH<sub>2</sub>Cl<sub>2</sub>; (iii) Hg(OAc)<sub>2</sub>, CH<sub>2</sub>Cl<sub>2</sub>, AcOH; (iv) P<sub>2</sub>S<sub>5</sub>, NaHCO<sub>3</sub>, 1,4-dioxane, heat; (v) NaOEt, THF, reflux, 15 min, then (*n*-Bu)<sub>4</sub>NBr and NiCl<sub>2</sub>·6H<sub>2</sub>O.

was obtained by treatment of **11** with sodium ethoxide (generating the dithiolate intermediate, as in Scheme 1), followed by the addition of tetrabutylammonium bromide and nickel(II) chloride. The product was obtained as a dark red solid in 81% yield.

A second type of electroactive ligand was used to prepare analogous complexes (Chart 1). Compound **13**<sup>22</sup> was subjected to the same procedure outlined in Scheme 1 to generate **14–17** in near quantitative yield (apart for **15**, which was isolated in 42% yield).

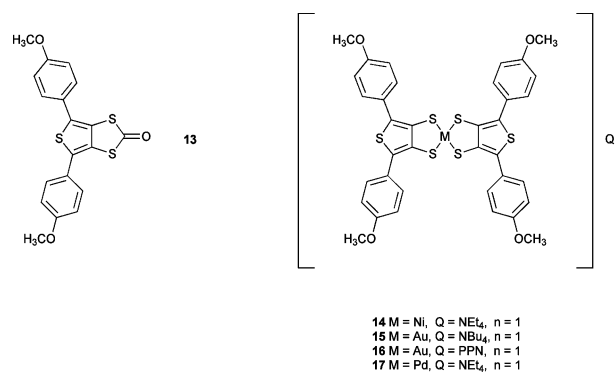


**Chart 1**

### X-Ray crystallography

The structure of **3** has been reported previously.<sup>21</sup> Green needles of compound **5** were grown from a THF–diethyl ether solution by slow evaporation. The asymmetric unit of **5** is shown in Fig. 1 and consists of two independent half-units with inversion centres at the gold atoms of the dithiolene units. The 5-membered rings within the dithiolene unit represented by Au(2)–S(8)–C(18)–C(19)–S(9) are essentially planar with a maximum deviation from the plane of 0.004(4) Å. In contrast, the equivalent unit, Au(1)–S(2)–C(6)–C(7)–S(3), is puckered with a maximum deviation of 0.108(4) Å. The terthiophene units adopt *anti-syn* conformations, in which the peripheral *anti* thiophene rings have short S...S contacts with neighbouring thiolate sulfurs of S(3)···S(5) = 3.358(3) Å and S(6)···S(8) = 3.149(3) Å. The shorter contact is associated with closer coplanarity between adjacent thiophene units and could be due to a higher degree of  $\pi$ -delocalisation; the torsion angles for C(7)–C(8)–C(9)–C(10) and C(15)–C(16)–C(17)–C(18) are 146.5(6)° and 161.24(6)°, respectively. The bithiophene units arranged in a *syn* conformation are also twisted, with torsion angles of C(3)–C(4)–C(5)–C(6) = 33.6(9)° and C(19)–C(20)–C(21)–C(22) = 39.3(9)°. The only significant intermolecular short contact is found for S(2)···S(10) (*x* + 1, *y*, *z*), in which the distance is 3.455(3) Å.

Dark red crystals of compound **12** were obtained by slow diffusion of diethyl ether or cyclohexane into a THF solution of the compound. In the case of this nickel complex, the terthiophene is composed of an all-*anti* conformation and in this case, the asymmetric unit contains half an anion, with an inversion centre at the metal atom (Fig. 2). Intramolecular short contacts within adjacent thiophenes exist for S(1)···S(4) (3.159(1) Å) and S(2)···S(5) (3.198(2) Å). The torsion angles between terminal thiophenes and the central heterocycle are 164.2(2)° for C(4)–C(5)–C(6)–C(7) and 168.0(2)° for C(8)–C(9)–C(10)–C(11), whilst the maximum deviation from the plane for the central dithiolene

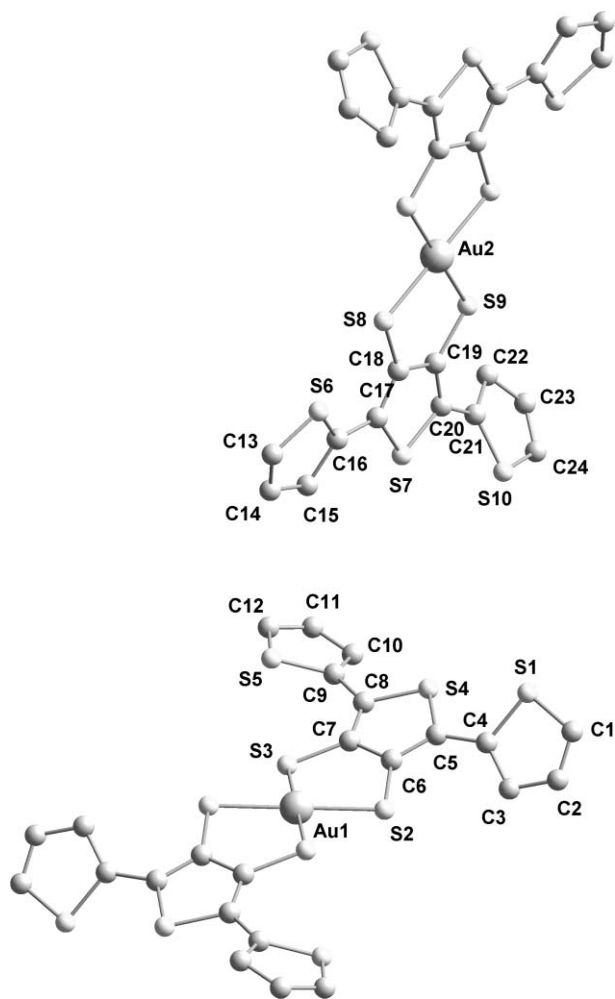


**Fig. 1** The structure of **5** with H atoms and PPN counterion omitted. Symmetry operations for the second half of each anion:  $1 - x, 1 - y, 1 - z$  for Au(1);  $-x, -y, -z$  for Au(2).

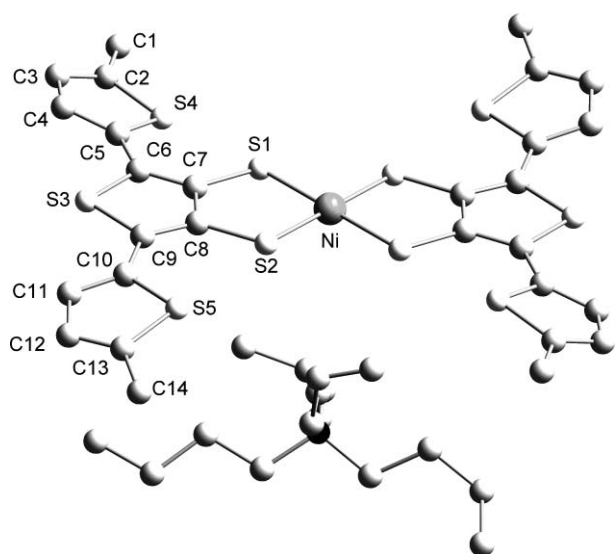


**Fig. 2** The structure of complex **12** with H atoms omitted. Symmetry operation for the second half of the anion:  $1 - x, 1 - y, 1 - z$ .

rings, Ni–S(1)–C(7)–C(8)–S(2), is 0.015 Å. Overall, these features portray a more nearly planar structure for **12**, compared to compound **5**.

Similar to that of **5**, the crystal structure of **16** (Fig. 3) also shows two independent half-units with inversion centres at the gold atoms. One methoxy functionality (O(4)–C(25)) shows disorder in its alignment with its adjacent benzene ring. The phenylene rings in both molecules are twisted in the same range as the thiophene units in **5**, with maximum torsion angles of 164.8(9)° (C(10)–C(4)–C(3)–C(2)) and 141.2(9)° (C(1)–C(11)–C(12)–C(18)) for the Au(1) molecule and 144.0(7)° (S(6)–C(29)–C(30)–C(31)) and 137.2(8)° (S(6)–C(20)–C(21)–C(22)) for the Au(2) molecule. Au(1) and Au(2) lie out of the plane formed by S(2)–Au(1)–S(1)–S(1')–S(2') and S(4')–S(5')–S(4)–S(5)–Au(2) by 0.8545(11) and 0.6517(10) Å, respectively (primes denote symmetry-equivalent atoms). Examining the planarity of the 5-membered rings in the dithiolene units for each of the complexes (**5**, **12** and **16**), the folding vectors along S...S show significant deviations in the Au complexes. Whereas the value for the nickel complex is 2.32(4)°, the relative folding vectors in **16** have angles of 10.8(2)° (Au(1) unit) and 12.8(2)° (Au(2) unit). Although the S...S folding vector in the Au(1) molecule of **5** is 24.02(12)°, the second molecule has a far smaller value, 2.25(12)°, demonstrating that a reasonably planar conformation is not exclusive to the Ni dithiolene unit.

### Electrochemistry

End-capped oligothiophenes are ideal model structures for the electrochemical characterisation of unsubstituted analogues, since the blocking groups inhibit chemical coupling processes during oxidation/reduction processes, enabling the observation of well-defined (and in most cases reversible) redox waves.<sup>23</sup> In this work, compound **12** has been used to evaluate the electroactivity of compound **3**. The cyclic voltammograms of both compounds are shown in Fig. 4 (see also Table 1 for data on all monomers and polymers). In our previous communication,<sup>21</sup> the redox wave centred at  $-0.13$  V for compound **3** was attributed to the oxidation of the nickel dithiolene unit ( $3^{2-} \rightleftharpoons 3^-$ ) and the position of this wave remains essentially unaltered in compound **12**. The reduction of the terthiophene units in **3** is shifted in **12** to a more negative potential (by 400 mV) as a result of the inductive effects of the four terminal methyl groups. The greatest difference between the electroactivity of the two compounds concerns the oxidation of the terthiophene units. Whereas **3** gives an irreversible peak at  $+0.46$  V (representing the onset of polymerisation), compound **12** displays three quasi-reversible oxidation waves at  $+0.30$ ,  $+0.70$  and  $+1.11$  V. The first of these oxidations represents the simultaneous oxidation of both terthiophene units and these processes can be resolved by square wave voltammetry (see inset in Fig. 4). A higher build up of positive charge and subsequent coulombic repulsion is responsible for the large difference in the third and fourth oxidation processes of the complex, which could be assigned to either the terthiophene units or the second oxidation of the nickel dithiolene.

The electron donating ability of the dithiolene systems is reduced in the palladium (**4**) and gold analogues (**5** and **6**). As for **3**, compound **4** displays two sequential oxidation processes but the potentials are raised by 0.26 and 0.16 V, respectively. The greater degree of  $\pi$ -delocalisation within the nickel complex is represented

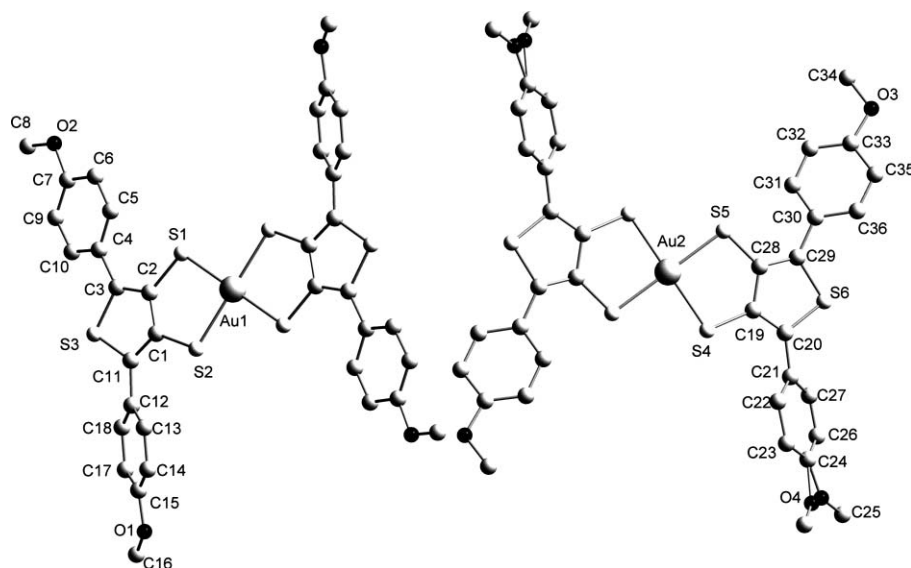


**Fig. 3** The structure of **16** with H atoms and PPN counterion omitted. Symmetry operations for the second half of each anion:  $1 - x, -y, 1 - z$  for Au(1);  $1 - x, 1 - y, -z$  for Au(2).

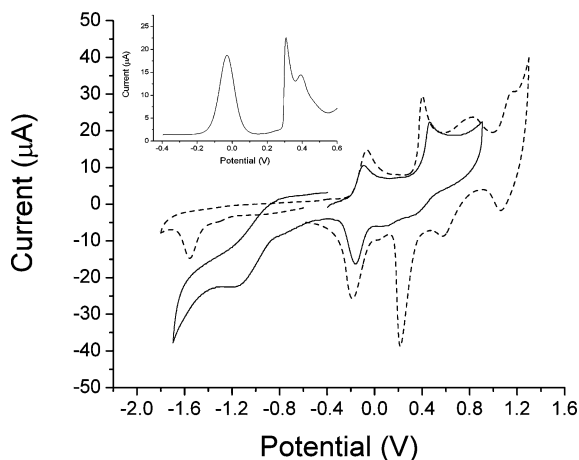


**Fig. 4** Cyclic voltammograms of compounds **3** (solid line) and **12** (dashed line) using glassy carbon working electrode, Ag/AgCl reference electrode and Pt counter electrode, in  $\text{CH}_2\text{Cl}_2$  (substrate  $ca. 10^{-3}$  M) at a scan rate of  $100 \text{ mV s}^{-1}$ . The inset shows the square wave voltammogram for compound **12** between  $-0.4$  and  $+0.6$  V.

by the reversibility and low potential for the first oxidation process. As stated above, the first reversible oxidation wave for compound **3** originates from the nickel dithiolene unit, but the irreversibility of the two oxidation processes in **4** should be due, in part, to the removal of electrons from at least one of the terthiophene units, since polymerisation takes place (see later). In the gold complexes **5** and **6**, which only vary in the nature of the more delocalised fragment which encompasses the anion, only one irreversible oxidation wave is observed at roughly the same potential and this is confidently assigned to the terthiophene ligand. For all monomer complexes, a single irreversible reduction wave is observed in the region  $-1.16$  to  $-1.40$  V.

Polymers of compounds **3–6** were grown electrochemically from solutions of the corresponding monomers ( $ca. 10^{-3}$  M in  $\text{CH}_2\text{Cl}_2$ ) by repetitive cycling over the range  $0.0$  to  $+1.3$  V on gold or indium tin oxide (ITO) glass working electrodes (representative traces are shown in Fig. 5). In each case, the growth of a fresh oxidation wave represents the emerging electrochemical signature of the new polymeric material. Once the polymer films were established, the coated working electrodes were removed from the monomer solution, washed with dichloromethane and placed in a monomer-free acetonitrile solution containing  $0.1$  M

**Table 1** Electrochemical<sup>a</sup> and absorption spectroscopy data<sup>b</sup> for compounds **3–6**, poly(**3**), poly(**4**), poly(**5**) and poly(**6**)

Compound	$E_{\text{ox}}/\text{V}$	$E_{\text{red}}/\text{V}$	$\lambda_{\text{max}}/\text{nm}$
<b>3</b>	$-0.13$ (70) <sup>c</sup> , $+0.46$ <sup>d</sup>	$-1.16$ <sup>d</sup>	340, 391, 480, 530
<b>4</b>	$+0.13$ <sup>d</sup> , $+0.30$ <sup>d</sup>	$-1.40$ <sup>d</sup>	300, 321(sh), 440, 477(sh)
<b>5</b>	$+0.57$ <sup>d</sup>	$-1.25$ <sup>d</sup>	266, 306, 391
<b>6</b>	$+0.60$ <sup>d</sup>	$-1.25$ <sup>d</sup>	259, 308, 390
<b>12</b>	$-0.12$ (120) <sup>c</sup> , $+0.30$ (190) <sup>c</sup> , $+0.70$ (240) <sup>c</sup> , $+1.11$ (80) <sup>c</sup>	$-1.56$ <sup>d</sup>	342, 394, 478, 527
poly( <b>3</b> )	$+0.04$ <sup>d</sup> , $+0.66$ (10) <sup>c</sup> , $+0.97$ (80) <sup>c</sup>	$-1.04, -1.26$	492, 908
poly( <b>4</b> )	$+0.12$ (60) <sup>c</sup> , $+0.27$ (100) <sup>c</sup>	—	514 (717) <sup>c</sup>
poly( <b>5</b> )	$+0.32$ (250) <sup>c</sup> , $+0.85$ (160) <sup>c</sup>	—	405, 494 (647) <sup>c</sup>
poly( <b>6</b> )	$+0.30$ (90) <sup>c</sup> , $+0.80$ (50) <sup>c</sup>	—	412, 497 (665) <sup>c</sup>

<sup>a</sup> Data obtained from cyclic voltammetry experiments conducted in  $\text{CH}_2\text{Cl}_2$  vs Ag/AgCl for monomers and on ITO glass in acetonitrile for polymers.

<sup>b</sup> Experiments carried out in  $\text{CH}_3\text{CN}$  solution for molecular species and solid state on ITO glass for the polymers. <sup>c</sup> Figures in parentheses represent  $\Delta E_{\text{pa-pc}}$  in mV. <sup>d</sup> Irreversible peak. <sup>e</sup> Onset of longest wavelength absorption band.

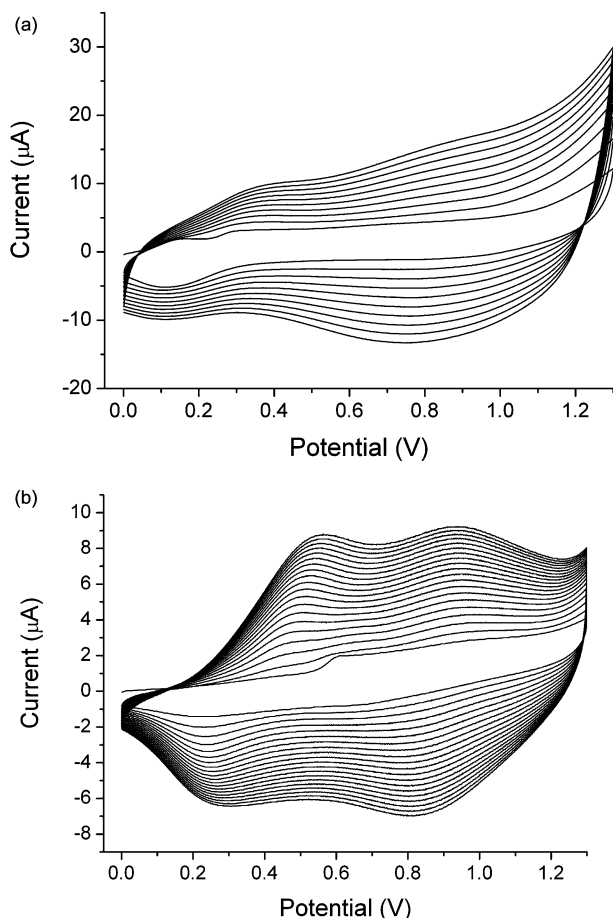


**Fig. 5** Electrochemical growth of poly(4) (top) and poly(5) (bottom) in  $\text{CH}_2\text{Cl}_2$ ; monomer concentration *ca.*  $10^{-3}$  M,  $100 \text{ mV s}^{-1}$ , vs Ag/AgCl.

$\text{NBu}_4\text{PF}_6$ . The cyclic voltammograms of each of the polymers of compounds **4–6** gave two reversible or quasi-reversible oxidation waves, in contrast to the single irreversible oxidation peaks of the corresponding monomers (Fig. 6). In poly(4), the oxidation peaks were approximately 0.2 and 0.6 V lower than the gold-containing polymers. For the Pd- and Au-containing materials, the two reversible/quasi-reversible oxidation processes are assigned

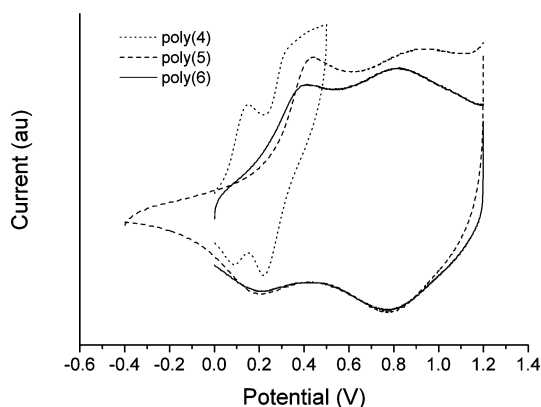


**Fig. 6** Cyclic voltammograms of poly(4), poly(5) and poly(6) films on Au in monomer-free acetonitrile solution containing 0.1 M *n*-Bu<sub>4</sub>PF<sub>6</sub>, scan rate  $100 \text{ mV s}^{-1}$ , vs Ag/AgCl.

exclusively to the polythiophene chains, since there is no metal-centred electroactivity evident in monomers **4–6** and none is expected in the related polymer structures. Poly(4), poly(5) and poly(6) have poor stability under n-doping and the polymers are lost from the electrode at negative potentials (less than  $-1.0$  V) as a result of chemical degradation or dissolution from the electrode surface.

The electroactivity of poly(3) is surprising in that the reversibility of the nickel dithiolene-centred oxidation is lost and the process is raised by 170 mV (compared to the monomer).<sup>21</sup> Indeed, the oxidation processes associated with the polythiophene chains are higher than those for the palladium- and gold-containing polymers; this is due to the increase of positive charge located at the oxidised metal centres in poly(3), which will lower the electron density of the polythiophene ligand.

### Electronic absorption spectroscopy

Absorption data and, in particular, UV-vis spectroelectrochemistry, provide a deeper insight into the electronic properties of the polymers. The electronic spectrum of the polymer grown on ITO glass, along with spectra of **3** at  $-0.40$  and  $+0.25$  V in MeCN, are shown in Fig. 7. A fresh solution of the monomer gives an identical spectrum to that obtained from a solution of **3** at  $-0.4$  V (spectroelectrochemistry was conducted using an optically transparent thin-layer electrochemical (OTTLE) cell). The complex oxidises after several days under ambient conditions, giving a spectrum that can be reproduced spectroelectrochemically at  $+0.25$  V and which features an additional absorption peak at 917 nm, corresponding to the oxidised nickel dithiolene monoanion species.<sup>8</sup> In both oxidation states, the peaks at 335 and 342 nm correspond to a  $\pi$ - $\pi^*$  transition within the triaryl units, as seen for similar terthiophene systems.<sup>6</sup> For the polymer film, this transition is shifted bathochromically by *ca.* 150 nm, indicative of an increase in conjugation and providing further proof for the generation of a polymeric material. The peak for the monoanion dithiolene system remains at 908 nm, indicating that, under the electrochemical conditions employed, this is the preferred ground state of the polymer. However, it should be noted that a neutral dithiolene may also show an absorption in this part of the spectrum. The most remarkable feature of poly(3) is the extremely broad absorption of the material between 400 and 1000 nm. Conjugated polymers that cover such a vast range are extremely rare; since the maximum

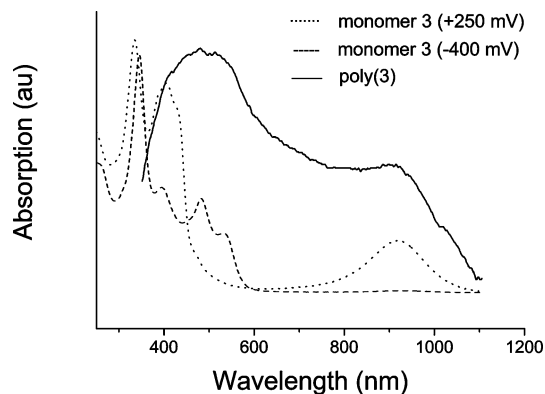


**Fig. 7** Electronic absorption spectra for **3** in MeCN and poly(3) as a thin film on ITO glass.

of the photon flux of the sun peaks around 700 nm (just out of the range of most conjugated polymers such as simple PPVs and polythiophenes), low band-gap polymers such as poly(3) could be extremely useful materials as light-harvesting components in plastic photovoltaic devices.<sup>9</sup>

The spectroelectrochemical plot of **12** is shown in Fig. 8 and should be considered alongside the electrochemical data depicted in Fig. 4 and summarised in Table 1. A dramatic change in absorption characteristics is observed once the potential exceeds 0.0 V, coinciding with the first oxidation process of the compound (the spectroelectrochemical experiment was conducted on the material as a thin film, hence the small difference in potentials). Peaks at 478 and 527 nm diminish rapidly and strong fresh peaks emerge at 404 and 434 nm. Concurrently, the signature of the dithiolene monoanion arises at 914 nm. Above +0.8 V the film of compound **12** begins to fall away from the electrode, due to the high solubility of the multicharged intermediate. Since the complication of coupling reactions between oxidised units (*i.e.* polymerisation) has been eliminated from compound **12** by the end-capping methyl groups, we benefit from well-defined absorption spectra that can be ascribed irrefutably to the characteristics of stable charged intermediates. From the spectroelectrochemical plot and the discussion above, we can conclude that the oxidised state of monomer **3**, which persists in solution after several days, is in fact the multi-oxidised species with electrons removed from the Ni dithiolene unit and the terthiophene segments (Fig. 7). During the oxidation of **3**, repetitive cycling (0.0 to +1.3 V) is required for the cation radical intermediates to trap and dimerise to form poly(3).

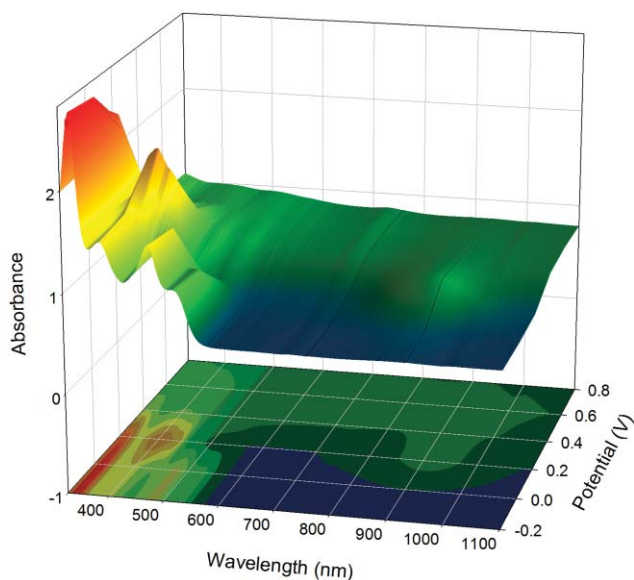


**Fig. 8** UV-vis spectroelectrochemical plot for compound **12** deposited on ITO glass in dichloromethane solution.

The spectroelectrochemical plot for poly(5) is shown in Fig. 9 (bottom) and represents the general absorption characteristics of the Pd- and Au-containing polymers. In these materials, the longest wavelength absorption peaks diminish over the first oxidation process and at higher potentials (>+0.4 V) the emergence of a band at *ca.* 1050 nm represents the generation of polarons/bipolarons in the polythiophene chains. The

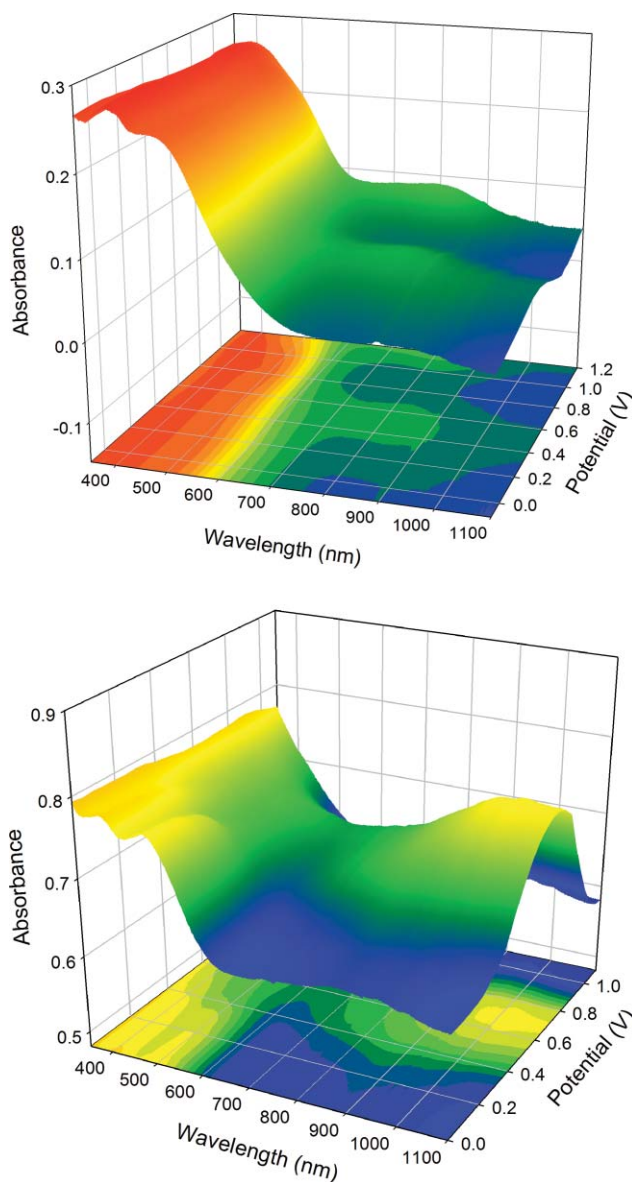


**Fig. 9** UV-vis spectroelectrochemical plot for poly(3) (top) and poly(5) (bottom) deposited on ITO glass in dichloromethane solution.

changes in absorption characteristics are similar to related poly(terthiophene)s,<sup>17,18,24</sup> hence we can conclude that there is no electronic contribution from the metal centres in poly(4), poly(5) and poly(6). Fig. 9 (top) shows the spectroelectrochemical spectrum for poly(3) and there is negligible change until the second oxidation wave is encountered at *ca.* +0.3 V. The emerging peak at 850 nm is lost at higher potential, specifically between the two reversible oxidation peaks (+0.66 and +0.97 V, Table 1), and a new broad band forms at 800 nm. Interestingly, the main  $\pi$ - $\pi^*$  band of the polythiophene chain is unchanged upon doping, indicating that the charged species are more localised within the dithiolene unit than the polymer main chain. The behaviour of poly(3) is very different from the electronic characteristics displayed by poly(5) upon oxidation and it is difficult to assign the electronic processes accurately because of the complex redox behaviour of poly(3). Indeed, compound **12** undergoes at least

four oxidation processes up to +1.2 V, providing a good model for the redox activity observed in the corresponding polymer. Thus, it can be assumed that the spectroelectrochemical behaviour of poly(**3**) arises from the oxidation of both nickel dithiolene and thiophene units, with the charged intermediates delocalised mainly over the metal dithiolene segments.

### Charge transfer materials

Dithiolenes **14–17** were isolated as the monoanionic species *via* the spontaneous oxidation of the dianion intermediates. The stability of the dianions are therefore very different from dithiolenes **3–6**, demonstrating the increased electron-donating properties of the methoxyphenylene-based ligands. This type of spontaneous oxidation has been observed in other Ni dithiolene complexes.<sup>25–27</sup> In an attempt to isolate crystalline molecular charge transfer materials, compounds **14–17** were oxidised under electrochemical and chemical conditions. Cyclic voltammetry showed that the redox properties of compounds **14–17** varied greatly. The nickel derivative gives the expected Ni-centred oxidation at  $-0.25$  V (quasi-reversible), and is accompanied by two further irreversible oxidations ( $+0.15$  V and  $+0.44$  V). Compared to complex **3**, the lower oxidation potential of **14** is attributed to the increased electron-donating properties of the *p*-methoxyphenylene groups, compared with the thiophenes in **3**. The gold complexes are reversibly oxidised at higher potentials (*ca.*  $+0.6$  V) and undergo reduction at *ca.*  $-1.1$  V (irreversible). In contrast, the Pd analogue was not oxidised within the potential window applied (up to  $+1.2$  V), but underwent two irreversible reductions at  $-0.25$  V and  $-0.73$  V. In view of the above, it was not surprising that only the nickel complex (**14**) gave charge transfer materials upon chemical oxidation. Chemical oxidation was achieved by mixing **14** with a solution of the tetrathiafulvalene-based salt  $(\text{TTF})_3(\text{BF}_4)_2$ . Elemental analysis of the black product gave the formula  $(\text{TTF})_4[\text{Ni}\{\text{S}_2\text{C}_4\text{S}(\text{SC}_6\text{H}_4\text{OCH}_3)_2\}_2]_3$  and the material had a conductivity of  $9 \times 10^{-6}$  S  $\text{cm}^{-1}$ .

Electrocrystallisation from solutions of **14** and **16** in acetonitrile gave black microcrystalline powders. Elemental analyses indicated that there was very little counteranion ( $\text{NET}_4$  or PPN) present in the solids. The conductivities of the electrochemically oxidised materials were found to be  $2 \times 10^{-7}$  S  $\text{cm}^{-1}$  for the product of **14** and  $7 \times 10^{-8}$  S  $\text{cm}^{-1}$  for that of oxidised **16**.

### Conclusion

Novel and stable metal dithiolene complexes have been prepared and isolated in good yields. The structures incorporate redox-active units fused to the ligands and terthiophene analogues can be readily polymerised electrochemically to form films of the corresponding cross-linked poly(thiophenes). Electrochemical and UV-vis spectroelectrochemical experiments have been conducted on the polymers and the model compound **12**. The nickel dithiolenes show complex electrochemical behaviour involving both the metal dithiolene fragment and the terthiophene/poly(thiophene) chains. This is not the case for Pd and Au analogues, in which electroactivity is confined to the polymer backbone.

## Experimental

### General procedures and materials

All reactions and product manipulations were performed under an atmosphere of argon using standard Schlenk techniques. THF was dried over and distilled from Na. Melting points were taken using Gallenkamp Melting Point apparatus.  $^1\text{H}$  and  $^{13}\text{C}$  NMR spectra were collected on Varian UNITY-300 or Bruker ARX-300 spectrometers (chemical shifts are in ppm, coupling constants are in Hz), IR spectra were measured with a Perkin-Elmer 883 or Perkin-Elmer FT-IR Spectrum One using KBr pellets, UV-vis spectra of 0.1 mM solutions in a 1 cm cuvette were measured with a UNICAM UV 300 and mass spectra were collected with V.G. Autoespec, Micromass Trio 2000 or Kratos concept 1S instruments. Elemental analyses were obtained on a Perkin Elmer 240B/2400B or a Carlo Erba Instruments EA1108 elemental analyser.  $\text{NBu}_4[\text{AuBr}_2]$ ,<sup>28</sup>  $\text{PPN}[\text{AuCl}_2]$ ,<sup>28</sup>  $\text{Na}_2[\text{PdCl}_4]$ ,<sup>29</sup>  $(\text{TTF})_3(\text{BF}_4)_2$ <sup>30</sup> were synthesized by literature procedures. Conductivity measurements were carried out using the compressed pellet, two-probe method.<sup>31</sup>

### X-Ray crystallography

The data collection and refinement parameters of structures **5**, **12** and **16** are presented in Table 2. X-Ray diffraction data for compounds **5** and **16** were collected on a Bruker-Nonius KappaCCD area detector situated at the window of a rotating anode [ $\lambda(\text{Mo-K}\alpha) = 0.71073$  Å]. Data for compound **12** were collected at Daresbury SRS station 9.8 ( $\lambda = 0.6868$  Å). The structures were solved by direct methods and refined using programs of the SHELX family.<sup>32</sup> Hydrogen atoms were included in the refinement, but their displacement parameters and positions were constrained to ride on the atoms to which they are bonded. The data were corrected for absorption effects using SADABS.<sup>33</sup> The PLATON SQUEEZE<sup>34</sup> algorithm was applied to **16** to model the diffuse contribution from a highly disordered solvent of crystallisation to the electron density.

CCDC reference numbers 675707–675709. For crystallographic data in CIF or other electronic format see DOI: 10.1039/b801187g

### Cyclic voltammetry

Measurements were performed on a CH Instruments 660A Electrochemical Workstation with *iR* compensation, using anhydrous dichloromethane as the solvent, aqueous Ag/AgCl as the reference electrode and platinum wire and gold disk as the counter and working electrodes, respectively. All solutions were degassed (Ar) and contained the substrate in concentrations of *ca.*  $10^{-3}$  M, together with *n*- $\text{Bu}_4\text{NPF}_6$  (0.1 M) as the supporting electrolyte.

### Syntheses

$[\text{NBu}_4]_2[\text{Ni}\{\text{S}_2\text{C}_4\text{S}(\text{SC}_6\text{H}_3)_2\}_2]$  **3**. To a solution of **1** (0.1 g, 0.3 mmol) in dry THF (30 ml) under  $\text{N}_2$  was added NaOEt (0.5 M, 2.4 ml, 1.2 mmol) and the reaction was refluxed for 15 min.  $\text{Bu}_4\text{NBr}$  (0.1 g, 0.3 mmol) was then added followed by  $\text{NiCl}_2 \cdot 6\text{H}_2\text{O}$  (0.04 g, 0.15 mmol). The mixture was stirred overnight. The solvent was reduced *in vacuo* (5 ml), and diethyl ether was used to precipitate **3** as a dark red solid (0.17 g, 50%). Dark red crystals were obtained from a hexane–THF solution. Found: C, 56.37; H, 7.00; N, 2.31%.

**Table 2** The data collection and refinement parameters of complexes **5**, **12** and **16**

	<b>5</b>	<b>12</b>	<b>16</b>
Empirical formula	C <sub>60</sub> H <sub>42</sub> AuNP <sub>2</sub> S <sub>10</sub>	C <sub>60</sub> H <sub>32</sub> N <sub>2</sub> NiS <sub>10</sub>	C <sub>73</sub> H <sub>58</sub> AuNO <sub>4</sub> P <sub>2</sub> S <sub>6</sub>
Formula weight	1356.45	1220.67	1452.46
Crystal system	Triclinic	Monoclinic	Triclinic
Space group	<i>P</i> $\bar{1}$	<i>P</i> 2 <sub>1</sub> / <i>c</i>	<i>P</i> $\bar{1}$
<i>a</i> /Å	14.2162(1)	8.7090(7)	11.101(3)
<i>b</i> /Å	14.6583(2)	21.2066(16)	15.888(4)
<i>c</i> /Å	15.0674(2)	17.7517(13)	19.945(5)
<i>a</i> /°	76.383(1)		105.418(4)
<i>β</i> /°	80.037(1)	103.521(2)	100.449(4)
<i>γ</i> /°	65.190(1)		99.858(4)
<i>V</i> /Å <sup>3</sup>	2760.10(6)	3187.7(4)	3244.5(13)
<i>Z</i>	2	2	2
<i>μ</i> /mm <sup>-1</sup>	3.143	0.670	2.560
<i>T</i> /K	120	120	120
Crystal size/mm	0.42 × 0.10 × 0.04	0.10 × 0.08 × 0.05	0.38 × 0.18 × 0.11
<i>θ</i> <sub>max</sub> /°	27.45	23.81	23.30
Reflections collected	38561	22238	14816
Independent reflections	12263	5371	9255
<i>R</i> <sub>int</sub>	0.0442	0.0183	0.0331
Refined parameters	671	343	785
<i>R</i> ( <i>F</i> , <i>F</i> <sup>2</sup> > 2σ)	0.0434	0.0306	0.0483
<i>R</i> <sub>w</sub> ( <i>F</i> <sup>2</sup> , all data)	0.1178	0.0805	0.1120
Goodness of fit ( <i>F</i> <sup>2</sup> )	1.027	1.044	0.945
Difference map extremes/e Å <sup>-3</sup>	2.21, -2.55	0.69, -0.25	2.66, -1.36

C<sub>56</sub>H<sub>84</sub>NiN<sub>2</sub>S<sub>10</sub> requires: C, 57.78; H, 7.22; N, 2.40%. *δ*<sub>H</sub> (CDCl<sub>3</sub>): 7.25 (m, 4H), 6.98 (br, 4H), 6.88 (br, 4H), 3.6 (br, 16H), 1.7 (m, 16H), 1.35 (m, 16H), 0.83 (t, 24H, *J* = 6.87). *m/z* (FAB<sup>-</sup>) 678.

[NEt<sub>4</sub>]<sub>2</sub>[Pd{S<sub>2</sub>C<sub>4</sub>S(SC<sub>4</sub>H<sub>3</sub>)<sub>2</sub>}<sub>2</sub>] **4**. To a solution of **1** (0.1 g, 0.3 mmol) in dry THF (30 ml) under N<sub>2</sub> was added NaOEt (0.5 M, 2.4 ml, 1.2 mmol) and the reaction was refluxed for 15 min. Et<sub>4</sub>NBr (0.06 g, 0.3 mmol) was then added, followed by Na<sub>2</sub>[PdCl<sub>4</sub>] (0.04 g, 0.15 mmol). The mixture was stirred overnight. The compound was collected by filtration to afford **4** as a brown solid and washed with copious amounts of water to eliminate excess Et<sub>4</sub>NBr (0.16 g, 49%). Found: C, 44.79; H, 4.61; N, 2.38%. C<sub>32</sub>H<sub>32</sub>PdN<sub>2</sub>S<sub>10</sub> requires: C, 44.90; H, 3.72; N, 1.64%. *δ*<sub>H</sub> (DMSO): 7.5 (q, 8H, *J* = 9.1 and 5.1), 7.0 (t, 4H, *J* = 4.4), 3.2 (q, 12H, *J* = 9.1 and 6.9), 1.2 (t, 8H, *J* = 6.9). Mp 230–232 °C. *m/z* (FAB<sup>-</sup>) 725.

[PPN][Au{S<sub>2</sub>C<sub>4</sub>S(SC<sub>4</sub>H<sub>3</sub>)<sub>2</sub>}<sub>2</sub>] **5**. To a solution of **1** (0.1 g, 0.3 mmol) in dry THF (30 ml) under N<sub>2</sub> was added NaOEt (0.5 M, 2.4 ml, 1.2 mmol) and the reaction was refluxed for 15 min. PPN[AuCl<sub>4</sub>] (0.13 g, 0.15 mmol) was then added and the mixture was stirred overnight. The solvent was removed under reduced pressure to afford **5** as a green solid, which was purified from a THF–diethyl ether solution (0.15 g, 38%). Found: C, 52.27; H, 2.79; N, 0.98%. C<sub>60</sub>H<sub>42</sub>AuNP<sub>2</sub>S<sub>10</sub> requires: C, 53.11; H, 3.10; N, 1.03%. *δ*<sub>H</sub> (CDCl<sub>3</sub>): 7.52 (m, 10H), 7.35 (m, 20H), 7.24 (dd, 4H, *J* = 1.2 and 3.6), 7.11 (dd, 4H, *J* = 1.2 and 5.4), 6.94 (dd, 4H, *J* = 3.6 and 5.4). Mp 143–145 °C. *m/z* (FAB<sup>-</sup>) 816.

[NBu<sub>4</sub>][Au{S<sub>2</sub>C<sub>4</sub>S(SC<sub>4</sub>H<sub>3</sub>)<sub>2</sub>}<sub>2</sub>] **6**. To a solution of **1** (0.1 g, 0.3 mmol) in dry THF (30 ml) under N<sub>2</sub> was added NaOEt (0.5 M, 2.4 ml, 1.2 mmol) and the reaction was refluxed for 15 min. *n*-Bu<sub>4</sub>N[AuBr<sub>4</sub>] (0.08 g, 0.15 mmol) was then added and the mixture was stirred overnight. The solvent was removed under reduced pressure to afford **6** as a green solid, which was purified from a THF–diethyl ether solution (0.14 g, 55%). Found: C, 40.79; H, 3.88; N, 1.13%. C<sub>40</sub>H<sub>48</sub>AuNS<sub>10</sub> requires C, 45.31; H, 4.56; N, 1.32%.

*δ*<sub>H</sub> (CDCl<sub>3</sub>): 7.4 (dd, 4H, *J* = 5.4 and 1.2), 7.3 (dd, 4H, *J* = 3.8 and 1.2), 7.1 (dd, 4H, *J* = 5.4 and 3.8), 3.4 (m, 8H), 1.8 (m, 8H), 1.4 (m, 8H), 0.9 (t, 12H, *J* = 7.2). Mp 227–229 °C. *m/z* (FAB<sup>-</sup>) 816.

**4,5-Bis(5-methyl-2-thienylhydroxymethyl)-1,3-dithiole-2-thione 8 and 4,5-bis(5-methyl-2-thienoyl)-1,3-dithiole-2-thione 9**. Under an inert atmosphere of N<sub>2</sub>, vinylenetrithiocarbonate **7** (2.50 g, 18.66 mmol) was dissolved in dry THF (75 ml) and cooled to -78 °C. To this solution, lithium diisopropylamide monotetrahydrofuran (LDA·THF) (1.5 M solution in cyclohexane, 13.7 ml, 20.53 mmol) was added and the reaction left to stir for approximately 20 min. Then 5-methyl-2-thiophenecarboxaldehyde (2.21 ml, 20.53 mmol) was added and the mixture stirred for 10 min. LDA·THF was added again (13.7 ml, 20.53 mmol) and stirring continued for 15 min, which was then followed by the addition of another portion of 5-methyl-2-thiophenecarboxaldehyde (2.21 ml, 20.53 mmol) and left to stand for 5 min before being allowed to warm to room temperature. The reaction mixture was poured into saturated sodium bicarbonate solution (until the precipitate was dissolved) and the organic layer separated. The aqueous phase was then extracted with dichloromethane, the organic extracts combined and dried over MgSO<sub>4</sub>, and the solvent was removed under reduced pressure. The residue was purified by column chromatography (silica, dichloromethane and then ethyl acetate) to afford the mono- and the diol **8** respectively in order of elution. The diol was obtained as an unstable red oil, which was reacted immediately (5.61 g). The diol (5.61 g) was dissolved in dichloromethane (125 ml) and to this a ten-fold excess (w/w) of manganese(IV) oxide (56 g) was added portionwise and the mixture stirred for 2 min at room temperature and immediately filtered through a layer of silica (*ca.* 10 cm thick) in a fritted filter funnel, eluting with dichloromethane. The solvent was removed under reduced pressure to afford compound **9** as an orange tar,

which gradually solidified upon standing (4.77 g, 67% from **7**).  $\delta_{\text{H}}$  (CDCl<sub>3</sub>): 7.54 (2H, d,  $J = 3.9$ ), 6.78 (2H, d,  $J = 3.9$ ), 2.51 (6H, s).  $\delta_{\text{C}}$  (CDCl<sub>3</sub>): 207.6, 175.1, 154.2, 144.0, 139.9, 136.3, 127.5, 16.2.  $m/z$  (CI) 383 [M + H]<sup>+</sup>.

**4,5-Bis(5-methyl-2-thienyl)-1,3-dithiole-2-one 10.** To a solution of **9** (2.84 g, 7.43 mmol) in a dichloromethane–glacial acetic acid mixture (3:1, v/v, 80 ml) was added mercury(II) acetate (3.31 g, 10.40 mmol) and the mixture stirred at room temperature overnight. The mixture was filtered through a layer of silica, eluting with dichloromethane. The filtrate was washed with water and a saturated sodium bicarbonate solution. The organic extracts were dried over MgSO<sub>4</sub> and the solvent was removed under reduced pressure to give a crude yellow solid. The solid was dissolved in a minimal amount of dichloromethane with heating and then petroleum ether (boiling range 40–60 °C) was added to precipitate the compound. A shiny yellow solid was obtained (1.95 g, 72%).  $\delta_{\text{H}}$  (CDCl<sub>3</sub>): 7.51 (2H, d,  $J = 3.9$ ), 6.77 (2H, d,  $J = 3.9$ ), 2.51 (6H, s).  $\delta_{\text{C}}$  (CDCl<sub>3</sub>): 187.3, 176.8, 153.9, 140.2, 136.3, 135.1, 127.4, 16.2.  $m/z$  (APCI+) 367 [M + H]<sup>+</sup>, 339 [M – CO + H]<sup>+</sup>.  $m/z$  (APCI–) 338 [M – CO + e]<sup>–</sup>.

**4,6-Bis(5-methyl-2-thienyl)thieno[3,4-*d*]-1,3-dithiole-2-thione 11.** A mixture of compound **10** (1.60 g, 4.37 mmol), phosphorus pentasulfide (9.71 g, 21.85 mmol) and sodium hydrogencarbonate (1.84 g, 21.85 mmol) in 1,4-dioxane (80 ml) was heated to 90 °C for 3 h. The reaction mixture was allowed to cool to room temperature before adding water portionwise (10 × 10 ml) (**Caution!** H<sub>2</sub>S and CO<sub>2</sub> evolution). The mixture was stirred overnight. The precipitate was filtered off and washed with hot water before dissolving in chloroform and drying over MgSO<sub>4</sub>. After filtration, the solution was stirred with decolourising charcoal for 30 min and then filtered through a layer of silica. The solvent was removed under reduced pressure to give terthiophene **11** as a yellow solid (1.28 g, 80%). Recrystallization was achieved by dissolving the compound in a minimal amount of chloroform with heating and then petroleum ether (boiling range 40–60 °C) was added. The suspension was placed in an ice bath and the precipitate was filtered and washed with petroleum ether. A yellow solid was obtained (0.83 g, 52%). Found: C, 48.83; H, 2.28; S, 44.49%. C<sub>15</sub>H<sub>10</sub>OS<sub>5</sub> requires: C, 49.19; H, 2.73; S, 43.73%.  $\delta_{\text{H}}$  (CDCl<sub>3</sub>): 6.99 (2H, d,  $J = 3.6$ ), 6.73 (2H, dd,  $J = 3.6$  and 1.1), 2.52 (6H, br s).  $\delta_{\text{C}}$  (CDCl<sub>3</sub>): 192.5, 141.2, 132.2, 126.4, 125.5, 125.1, 123.4, 15.4.  $m/z$  (CI) 367 [M + H]<sup>+</sup>.

**[NBu<sub>4</sub>]<sub>2</sub>Ni{S<sub>2</sub>C<sub>4</sub>S(SC<sub>5</sub>H<sub>5</sub>)<sub>2</sub>}<sub>2</sub> 12.** To a solution of the methyl-capped terthiophene **11** (0.25 g, 0.68 mmol) in dry tetrahydrofuran (50 ml) under N<sub>2</sub> was added NaOEt (0.5 M ethanol solution, 5.44 ml, 2.72 mmol) and the mixture was refluxed for 15 min. *n*-Bu<sub>4</sub>NBr (0.22 g, 0.68 mmol) was then added, followed by NiCl<sub>2</sub>·6H<sub>2</sub>O (0.081 g, 0.34 mmol). The reaction was stirred overnight. The mixture was filtered and the filtrate was reduced in volume, then petroleum ether (boiling range 40–60 °C) was added to precipitate compound **12** as a dark red solid (0.337 g, 81%). Dark red crystals were obtained by slow diffusion of diethyl ether or cyclohexane into a THF solution of the compound. Found: C, 58.06; H, 7.29; S, 25.84; N, 2.26%. C<sub>60</sub>H<sub>92</sub>N<sub>2</sub>NiS<sub>10</sub> requires: C, 59.10; H, 7.55; S, 26.26; N, 2.30%.  $\delta_{\text{H}}$  (CDCl<sub>3</sub>): 6.82 (4H, br s), 6.59 (4H, br s), 2.74 (12H, br s), 3.58 (16H, br s), 1.63 (16H, br s), 1.28 (16H, br s), 0.80 (24H, t,  $J = 6.4$ ).  $m/z$  (APCI–) 734 [M – 2*n*-Bu<sub>4</sub>N + e]<sup>–</sup>.

**[NEt<sub>4</sub>][Ni{S<sub>2</sub>C<sub>4</sub>S(*p*-OCH<sub>3</sub>C<sub>6</sub>H<sub>4</sub>)<sub>2</sub>}<sub>2</sub> 14.** To a solution of 4,6-bis(4-methoxyphenyl)-thieno[3,4-*d*]-1,3-dithiole-2-one<sup>20</sup> **13** (0.1 g, 0.25 mmol) in dry THF (25 ml) under argon was added 7.5 ml of NaEtO (0.1 M). The reaction was stirred until the solid was dissolved (no more than 40 min because the ketone starting material precipitates back). Then 0.125 mmol (26 mg) of [NEt<sub>4</sub>]Br followed by 0.125 mmol (30 mg) of NiCl<sub>2</sub>·6H<sub>2</sub>O were added. After 24 h an orange solid was filtered and washed with water (to remove the [NEt<sub>4</sub>]Br excess) (99%). Found: C, 58.97; H, 5.76; N, 1.70; S, 20.84%. C<sub>44</sub>H<sub>48</sub>NNiO<sub>4</sub>S<sub>6</sub> requires: C, 58.33; H, 5.30; N, 1.55; S, 21.21%.  $\nu_{\text{max}}$ /cm<sup>–1</sup>: 1605 (C=C) (KBr).  $\delta_{\text{H}}$  (CDCl<sub>3</sub>): 7.52 (8H, d,  $J = 7.8$  Hz), 6.99 (8H, d,  $J = 7.5$  Hz), 3.87 (12H, s), 3.34 (8H, m), 1.30 (12H, m).  $m/z$  (LSIMS–) 774 ([M]<sup>–</sup>, 38%), 458 (100%).

**(Q)[Au{S<sub>2</sub>C<sub>4</sub>S(*p*-OCH<sub>3</sub>C<sub>6</sub>H<sub>4</sub>)<sub>2</sub>}<sub>2</sub>] (Q = NBu<sub>4</sub> 15, PPN 16).** Complexes **15** and **16** were prepared by a procedure similar to **14** using NBu<sub>4</sub>[AuBr<sub>4</sub>] (0.125 mmol, 95 mg) and PPN[AuCl<sub>4</sub>] (0.125 mmol, 110 mg) respectively. For compound **15**, a blue solid was filtered off after 24 h (42%). For compound **16**, the solution was evaporated *in vacuo* to the point of crystallisation, whereupon diethyl ether (20 ml) was added to precipitate the product as a violet solid (99%).

**15.** Found: C, 54.44; H, 5.03; N, 1.63; S, 17.10%. C<sub>52</sub>H<sub>64</sub>AuNO<sub>4</sub>S<sub>6</sub> requires: C, 54.00; H, 5.54; N, 1.21; S, 16.62%.  $\nu_{\text{max}}$ /cm<sup>–1</sup> 1606 (C=C) (KBr).  $\delta_{\text{H}}$  (CDCl<sub>3</sub>): 7.72 (8H, d,  $J = 8.7$  Hz), 6.88 (8H, d,  $J = 8.4$  Hz), 3.75 (12H, s), 3.02 (8H, m), 1.40 (8H, m), 1.17 (8H, m), 0.79 (12H, m).  $m/z$  (LSIMS–) 913 ([M]<sup>–</sup>, 100%), 459 (72).

**16.** Found: C, 59.05; H, 3.55; N, 0.80; S, 12.82%. C<sub>72</sub>H<sub>58</sub>AuNO<sub>4</sub>P<sub>2</sub>S<sub>6</sub> requires: C, 59.51; H, 4.00; N, 0.96; S, 13.22%.  $\nu_{\text{max}}$ /cm<sup>–1</sup> 1606 (C=C) (KBr).  $\delta_{\text{H}}$  (CDCl<sub>3</sub>): **16**: 7.67 (8H, d,  $J = 9.1$  Hz), 7.49 (8H, d,  $J = 5.5$  Hz), 7.35 (22H, m), 6.81 (8H, d,  $J = 8.8$  Hz), 3.78 (12H, s).  $m/z$  (LSIMS–) 914 ([M]<sup>–</sup>, 100%), 556 (32).

**[NEt<sub>4</sub>][Pd{S<sub>2</sub>C<sub>4</sub>S(*p*-OCH<sub>3</sub>C<sub>6</sub>H<sub>4</sub>)<sub>2</sub>}<sub>2</sub> 17.** Complex **17** was prepared by a procedure similar to **14** using [NEt<sub>4</sub>]Br (17 mg, 0.125 mmol) and Na<sub>2</sub>[PdCl<sub>4</sub>] (37 mg, 0.125 mmol). The solvent was reduced *in vacuo* (5 ml) and diethyl ether was used to precipitate **17** (82%) as a brown solid which was washed with water. Found: C, 55.04; H, 5.22; N, 1.81; S, 19.80%. C<sub>44</sub>H<sub>48</sub>NO<sub>4</sub>PdS<sub>6</sub> requires: C, 55.44; H, 5.04; N, 1.47; S, 20.16%.  $\nu_{\text{max}}$ /cm<sup>–1</sup> 1605 (C=C) (KBr).  $\delta_{\text{H}}$  (DMSO): 7.98 (8H, d,  $J = 8.7$  Hz), 6.88 (8H, d,  $J = 8.8$  Hz), 3.76 (12H, s), 3.15–3.18 (8H, m), 1.00–1.12 (12H, m).  $m/z$  (LSIMS–) 822 ([M]<sup>–</sup>, 5%), 764 (4), 459 (20).

### Oxidation reactions of dithiolene complexes

**(A) Chemical oxidation with (TTF)<sub>3</sub>(BF<sub>4</sub>)<sub>2</sub>.** To a solution of the corresponding dithiolene complex (0.05 mmol) in MeCN (15 ml) was added 0.065 mmol (51 mg) of (TTF)<sub>3</sub>(BF<sub>4</sub>)<sub>2</sub> (1:1.3 ratio). The corresponding mixtures were stirred for 15 h and then the product was collected by filtration; in some cases it was necessary to concentrate the solution under reduced pressure.

**(TTF)<sub>4</sub>[Ni{S<sub>2</sub>C<sub>4</sub>S(SC<sub>6</sub>H<sub>4</sub>OCH<sub>3</sub>)<sub>2</sub>}<sub>2</sub>]<sub>3</sub> 14T.** Found: C, 50.40; H, 3.20; S, 29.87%. (C<sub>6</sub>H<sub>4</sub>S<sub>4</sub>)<sub>4</sub>(C<sub>36</sub>H<sub>28</sub>O<sub>4</sub>S<sub>6</sub>Ni)<sub>3</sub> requires: C, 50.37; H, 2.62; S, 29.05%. Conductivity  $\sigma$ : 9 × 10<sup>–6</sup> S cm<sup>–1</sup>.

**(B) Electrocrystallisation.** To one arm of the “H-shaped” electrolysis cell was added 0.04 mmol of the dithiolene (**14**, **16**), and a solution of [NEt<sub>4</sub>]ClO<sub>4</sub> (0.1 mmol) (**14**) or CIPPN (0.1 mmol) (**16**) in 10 ml of dry acetonitrile was added to both arms of the cell.

The device was left under argon and protected from light. After standing for 19 d with a constant current of 1.2  $\mu\text{A}$ , a feathered material was deposited on the platinum wire. The material was removed from the electrode and left to dry.

( $Q$ )[ $M\{S_2C_4S(SC_3H_5)_2\}_2$ ] ( $M = \text{Ni}$ ,  $Q = \text{NEt}_4$  14-*elec*;  $M = \text{Au}$ ,  $Q = \text{PPN}$  16-*elec*). 14-*elec*. Found: C, 54.21; H, 3.28; S, 24.14%. ( $\text{C}_8\text{H}_{20}\text{N}$ ) $_x$ ( $\text{C}_{36}\text{H}_{28}\text{NiO}_4\text{S}_6$ ) $_y$  ( $x:y = 0:1$ ) requires: C, 55.74; H, 3.63; S, 24.79%. Conductivity  $\sigma$ :  $2 \times 10^{-7} \text{ S cm}^{-1}$ ;

16-*elec*. Found: C, 47.92; H, 2.93; S, 20.83%. ( $\text{C}_{36}\text{H}_{30}\text{NP}_2$ ) $_x$ ( $\text{C}_{36}\text{H}_{28}\text{AuO}_4\text{S}_6$ ) $_y$  ( $x:y = 0:1$ ) requires: C, 47.31; H, 3.08; S, 21.04%. Conductivity  $\sigma$ :  $7 \times 10^{-8} \text{ S cm}^{-1}$ .

## Acknowledgements

The authors thank EPSRC for funding the UK National Crystallography Service, and STFC for access to synchrotron facilities.

## References

- 1 C. Moorlag, B. C. Sih, T. L. Stott and M. O. Wolf, *J. Mater. Chem.*, 2005, **15**, 2433–2436.
- 2 M. O. Wolf, *J. Inorg. Organomet. Polym.*, 2006, **16**, 189–199.
- 3 J. Roncali, *J. Mater. Chem.*, 1999, **9**, 1875–1893.
- 4 D. T. McQuade, A. E. Pullen and T. M. Swager, *Chem. Rev.*, 2000, **100**, 2537–2574.
- 5 S. J. Higgins, *Chem. Soc. Rev.*, 1997, **26**, 247–257.
- 6 V. G. Albano, M. Bandini, C. Moorlag, F. Piccinelli, A. Pietrangelo, S. Tommasi, A. Umani-Ronchi and M. O. Wolf, *Organometallics*, 2007, **26**, 4373–4375.
- 7 A. Deronzier and J. C. Moutet, *Coord. Chem. Rev.*, 1996, **147**, 339–371.
- 8 C. L. Kean and P. G. Pickup, *Chem. Commun.*, 2001, 815–816.
- 9 F. J. Martínez, B. González, B. Alonso, J. Losada, M. P. García-Armada and C. M. Casado, *J. Inorg. Organomet. Polym.*, 2008, **18**, 51–58.
- 10 P. G. Pickup, *J. Mater. Chem.*, 1999, **9**, 1641–1653.
- 11 T. Anjos, S. J. Roberts-Bleming, A. Charlton, N. Robertson, A. R. Mount, S. J. Coles, M. B. Hursthouse, M. Kalaji and P. J. Murphy, *J. Mater. Chem.*, 2008, **18**, 475–483.
- 12 T. L. Stott and M. O. Wolf, *Coord. Chem. Rev.*, 2003, **246**, 89–101.
- 13 J. Hjelm, E. C. Constable, E. Figgemeier, A. Hagfeldt, R. Handel, C. E. Housecroft, E. Mukhtar and E. Schofield, *Chem. Commun.*, 2002, 284–285.
- 14 R. Kato, *Chem. Rev.*, 2004, **104**, 5319–5346.
- 15 T. D. Anthopoulos, S. Setayesh, E. Smits, M. Colle, E. Cantatore, B. de Boer, P. W. M. Blom and D. M. de Leeuw, *Adv. Mater.*, 2006, **18**, 1900–1904.
- 16 K. L. Marshall, G. Painter, K. Lotito, A. G. Noto and P. Chang, *Mol. Cryst. Liq. Cryst.*, 2006, **454**, 47–79.
- 17 R. Berridge, P. J. Skabara, C. Pozo-Gonzalo, A. Kanibolotsky, J. Lohr, J. J. W. McDouall, E. J. L. McInnes, J. Wolowska, C. Winder, N. S. Sariciftci, R. W. Harrington and W. Clegg, *J. Phys. Chem. B*, 2006, **110**, 3140–3152.
- 18 R. Berridge, S. P. Wright, P. J. Skabara, A. Dyer, T. Steckler, A. A. Argun, J. R. Reynolds, W. H. Ross and W. Clegg, *J. Mater. Chem.*, 2007, **17**, 225–231.
- 19 C. Pozo-Gonzalo, T. Khan, J. J. W. McDouall, P. J. Skabara, D. M. Roberts, M. E. Light, S. J. Coles, M. B. Hursthouse, H. Neugebauer, A. Cravino and N. S. Sariciftci, *J. Mater. Chem.*, 2002, **12**, 500–510.
- 20 P. J. Skabara, I. M. Serebryakov, D. M. Roberts, I. F. Perepichka, S. J. Coles and M. B. Hursthouse, *J. Org. Chem.*, 1999, **64**, 6418–6424.
- 21 C. Pozo-Gonzalo, R. Berridge, P. J. Skabara, E. Cerrada, M. Laguna, S. J. Coles and M. B. Hursthouse, *Chem. Commun.*, 2002, 2408–2409.
- 22 T. Khan, J. J. W. McDouall, E. J. L. McInnes, P. J. Skabara, P. Frère, S. J. Coles and M. B. Hursthouse, *J. Mater. Chem.*, 2003, **13**, 2490–2498.
- 23 C. R. Mason, P. J. Skabara, D. Cupertino, J. Schofield, F. Meghdadi, B. Ebner and N. S. Sariciftci, *J. Mater. Chem.*, 2005, **15**, 1446–1453.
- 24 P. J. Skabara, R. Berridge, I. M. Serebryakov, A. L. Kanibolotsky, L. Kanibolotskaya, S. Gordeyev, I. F. Perepichka, N. S. Sariciftci and C. Winder, *J. Mater. Chem.*, 2007, **17**, 1055–1062.
- 25 N. Robertson, D. L. Parkin, A. E. Underhill, M. B. Hursthouse, D. E. Hibbs and K. M. A. Malik, *J. Mater. Chem.*, 1995, **5**, 1731–1734.
- 26 A. Charlton, A. E. Underhill, A. Kobayashi and H. Kobayashi, *J. Chem. Soc., Dalton Trans.*, 1995, 1285–1295.
- 27 C. A. S. Hill, A. Charlton, A. E. Underhill, K. M. A. Malik, M. B. Hursthouse, A. I. Karaulov, S. N. Oliver and S. V. Kershaw, *J. Chem. Soc., Dalton Trans.*, 1995, 587–594.
- 28 P. Braunstein and R. J. H. Clark, *J. Chem. Soc., Dalton Trans.*, 1973, 1845–1848.
- 29 G. B. Kauffman and J. H.-S. Tsai, *Inorg. Synth.*, 1966, **8**, 234.
- 30 F. Wudl, *J. Am. Chem. Soc.*, 1975, **97**, 1962–1963.
- 31 F. Wudl and M. R. Bryce, *J. Chem. Educ.*, 1990, **67**, 717–718.
- 32 G. M. Sheldrick, *Acta Crystallogr., Sect. A*, 2008, **64**, 112.
- 33 G. M. Sheldrick, *SADABS, Version 2.10*, Bruker AXS Inc., Madison, Wisconsin, USA, 2003.
- 34 P. v. d. Sluis and A. L. Spek, *Acta Crystallogr., Sect. A*, 1990, **46**, 194–201; A. L. Spek, *J. Appl. Crystallogr.*, 2003, **36**, 7.